Life Sciences 226 (2019) 107–116

Contents lists available at ScienceDirect

Life Sciences

journal homepage: www.elsevier.com/locate/lifescie

Progression of micturition dysfunction associated with the development of heart failure in rats: Model of overactive bladder

A.G. Mora[a], S.R. Furquim[a], S.P. Tartarotti[a], D.R. Andrade[a], S.C. Janussi[a], K. Krikorian[a], T. Rocha[a], C.F. Franco-Penteado[b,d], D.G. Priolli[a], F.B.M. Priviero[c], M.A. Claudino[a,*]

[a] Laboratory of Multidisciplinary Research, São Francisco University Medical School, Bragança Paulista, SP, Brazil
[b] Hematology and Hemotherapy Center, University of Campinas, Campinas, SP, Brazil
[c] Department of Physiology, Medical College of Georgia, Augusta University, Augusta, GA, USA
[d] Faculty of Medical Sciences, University of Campinas, Campinas, SP, Brazil

ARTICLE INFO

Keywords:
Overactive bladder
Detrusor muscle
Aortocaval fistula
Micturition
Heart failure

ABSTRACT

Heart failure (HF) has a strong association with the development of lower urinary tract symptoms, especially overactive bladder (OAB); although this condition remains poorly investigated. In this study, we assess the aortocaval fistula (ACF) model as a novel experimental model of micturition dysfunction, associated with HF, focused on the molecular and functional studies to evaluate the autonomic nervous system and urinary bladder remodeling. Male rats were submitted to ACF for HF induction. Echocardiography, cystometric, histomorphometry and molecular analysis, as well as concentration-response curves to carbachol and ATP and frequency-response curves to electrical field stimulation (EFS) were evaluated in Sham and HF (4- and 12-weeksendpoint) groups. Compared to SHAM, HF groups exhibited progressive increases in the left ventricle (LV) mass and fractional shortening which indicates cardiac dysfunction, although HF was characterized only after 12 weeks by the reduced ejection fraction. For micturition function, HF groups presented increased non-voiding contractions (NVC) and decreased bladder capacity; however, when comparing HF groups, these urinary parameters were significantly impaired over the weeks (12-weeks). The contractile responses induced by CCh, ATP and EFS were greater in detrusor muscle (DSM) from HF rats. mRNA expression for muscarinic receptors (M2 and M3) was higher in DSM only after 12 weeks of ACF, in addition to MMP9 and TGF-beta. Histomorphometric revealed increased urothelium thickness in both HF groups, whereas DSM thickness occurred only after 12 weeks. Thus, the ACF model induced cardiac dyfunction with progressive micturition dysfunction over the weeks, characterized by increased DSM contractile mechanisms as well as extracellular matrix remodeling in the urinary bladder, representing a useful tool to evaluate the OAB associated with HF.

1. Introduction

Heart failure (HF) is no longer considered an isolated heart disease, because it involves multiple systems and compensatory mechanisms, accompanied by high rates of morbidity and mortality [1,2]. According to updated data from the American Heart Association (AHA), HF affected approximately 5.1 million individuals in the United States between the years of 2007–2012 and estimates show that these rates will increase 46% by 2030 [3,4]. Several studies have demonstrated a complex relationship between HF and the development of lower urinary tract symptoms (LUTS) [5–7]. Epidemiological data have shown that approximately 30–50% of men and women with HF suffer from LUTS [6,8], among the symptoms we highlight the overactive bladder (OAB), which presents in approximately 57% of patients with HF [8]. Although LUTS is not one of the first issues for treating HF patients, urinary worries may have a negative influence on their quality of life [5].

The LUTS, such as urgency, incontinence, nocturia and OAB, are associated with failures of urine storage [9]. The neural circuits in the bladder and urethra, composed of somatic, sympathetic and parasympathic fibers, regulate the abilities of the lower urinary tract tostore and to release urine [10]. During the urine storage phase the bladder and urethra work as a functional unit [11], and a progressive increase in sympathetic activity releases noradrenaline, which activates β-adrenoceptors in the detrusor smooth muscle (DSM), causing bladder

* Corresponding author at: Laboratory of Multidisciplinary Research, São Francisco University (USF), Avenida São Francisco de Assis, 218 - Jardim São Jose, Bragança Paulista, SP 12916-900, Brazil.
E-mail address: mario.claudino@usf.edu.br (M.A. Claudino).

https://doi.org/10.1016/j.lfs.2019.04.017
Received 26 February 2019; Received in revised form 3 April 2019; Accepted 5 April 2019
Available online 06 April 2019

relaxation and contributing to the filling phase during the micturition cycle [12]. Moreover, sympathetic stimulation will also stimulate α1-adrenoceptors in the urethra to provide bladder outlet resistance and prevent involuntary leakage of urine [13]. When a storage limit is reached, the sympathetic activity is ceased, and the acetylcholine released from parasympathetic fibers activates the muscarinic receptors, promoting contraction in the DSM and emptying of the bladder [14]. In addition, non-cholinergic excitatory transmission mediated by ATP *via* purinergic receptors in DSM may also contribute to bladder contractions during the micturition cycle [15]. Moreover, several studies have shown that the overactive DSM is present in conditions of urine storage failure, either in experimental models [16,17] or in humans [18,19] and the understanding of the mechanisms underlying the DMS dysfunction and the control of the micturition cycle may be the key for treating failures of storage in the urinary bladder.

In addition, HF and OAB have common risk factors such as hypertension, obesity and *diabetes mellitus* [8,20]. Dysfunction in the autonomic nervous system, pelvic ischemia and changes in signaling pathways that regulate smooth muscle tone are pointed out as possible mechanisms in the development of OAB associated with overactive DSM in cardiovascular disease [21–23]. However, despite the high prevalence of LUTS in HF patients, few studies have evaluated the pathophysiological alterations of urinary bladder in HF.

HF experimental models in mammals have provided additional support for understanding the pathophysiological alterations in HF. The aortocaval fistula (ACF) model has been extensively used for studying the pathophysiology of volume-overload HF in rats [24,25]. The ACF model results in immediate hemodynamic changes and consequent activation of compensatory neurohormonal mechanisms [24] that contribute to changes in the cardiac and renal overload, inadequate blood supply and oxidative stress, which may be responsible for the development of LUTS [26,27].

Since HF is associated with increased oxidative stress, lower nitric oxide bioavailability and activation of compensatory neurohormonal mechanisms, we hypothesized that HF causes hemodynamic changes promoting an imbalance and leading to molecular and functional changes of the DSM, which contribute to the micturition dysfunction and LUTS. Therefore, the purpose of this study was to characterize the ACF rat model associated with HF as a novel experimental model of OAB, as well as to evaluate the LUTS pathogenesis in HF, exploring the molecular and morphofunctional changes as well as changes in the contractile mechanism of the DSM.

2. Materials and methods

2.1. Ethics statement

All experimental procedures in this study were carried out in accordance with the general ethical guidelines for animal use established by the Brazilian Society of Laboratory Animal Science (SBCAL) and EC Directive 86/609/EEC for Animal. The experimental protocols were reviewed and approved by the Ethics Committee in Animal Research of the São Francisco University Medical School (protocol number 001.06.11).

2.2. Animals

All experimental procedures were carried out in accordance with the Ethical Principles in Animal Research adopted by the Brazilian College for Animal Experimentation (COBEA) and followed the Guide for the Care and Use of Laboratory Animals. Male Sprague Dawley rats (250–280 g) housed with free access to water and standard chow were maintained on a 12 h light–dark cycle. For the experimental protocols the animals were subdivided into three groups: Sham group and heart failure groups (HF), at 4 and 12 weeks after the surgical procedure (HF 4 wks and HF 12 wks, respectively). For the sham group, after no changes were observed in the cardiac, cystometric and morphofunctional parameters, we used a single sham group.

2.3. Induction of heart failure in a rat model of chronic volume overload

Animals were anesthetized with a mixture of ketamine (50 μg/g) and xylazine (10 μg/g). HF was induced by surgical creation of an ACF to induce chronic volume overload (VO). Briefly, a ventral laparotomy was performed to expose the abdominal aorta and vena cava and both vessels were then occluded temporarily. A short-bevel 18 g needle 7 was inserted into the abdominal aorta and advanced through the medial wall into the vena cava, creating a shunt below the renal arteries. The aortic puncture site was sealed with cyanoacrylate. The musculature and skin incisions were closed by standard techniques with absorbable- and no absorbable suture, respectively [28]. At the end of the surgery, the animals received analgesic (flunixin meglumine, 2.5 mg/kg, sc; [29]).

2.4. Validation of the heart failure model

For the validation of the HF model and better evaluation of cardiac function, the animals were submitted to transthoracic echocardiography after 4 and 12 weeks of ACF induction. The animals were anesthetized with xylazine (10 μg/g) and ketamine (50 μg/g) administered intraperitoneally, afterwards the tricotomy of the thoracic region was performed and the animals were submitted to the echocardiography procedure. The equipment was used for the examination (Sono Site - M Turbo, Washington, USA). The parameters measured were: left ventricle (LV) mass, ejection fraction, LV fractional shortening, fractional shortening of the posterior wall LV and end systolic and diastolic volumes [30].

2.5. Cystometry

After 4 and 12 weeks, rats were anesthetized with a mixture of ketamine (50 μg/g) and xylazine (10 μg/g) administered intraperitoneally. The bladder was exposed and a butterfly cannula (25 G) was inserted into the bladder. The cannula was connected to a pressure transducer and to an infusion pump through a catheter (PE50). Before starting cystometry the bladder was emptied. Continuous cystometry was performed by infusing saline into the bladder at a rate of 0.06 mL/min. The parameters measured were as follow: Basal pressure, threshold pressure (intravesical pressure immediately before micturition), voiding pressure (the peak pressure reached during micturition), capacity (volume of saline needed to induce the first micturition), voiding contractions frequency (number of voids per minute) and non-voiding contractions frequency (NVCs). NVCs were defined as spontaneous bladder contractions > 4 mm Hg from the baseline pressure that did not result in micturition [31].

2.6. Functional studies in detrusor muscle

After 4 and 12 weeks of ACF induction, animals were anesthetized with isoflurane and exsanguinated. After median laparotomy the urinary bladder was removed, sectioned into two longitudinal strips and maintained in Krebs-Henseleit solution containing: NaCl, 118 mM; $NaHCO_3$, 25 mM; glucose, 5.6 mM; KCl, 4.7 mM; KH_2PO_4, 1.2 mM; $MgSO_4$ $7H_2O$, 1.17 mM and $CaCl_2$ $2H_2O$, 2.5 mM. Each strip was mounted under resting tension of 10 mN in 10-ml organ chambers containing Krebs solution at 37° C (pH 7.4) and continuously bubbled with a mixture of 95% O_2 and 5% CO_2. The equilibration period was 60 min before starting the experiments. Isometric force was recorded using a PowerLab 400TM data acquisition system (Software Chart, version 7.0, AD Instrument, MA, USA). Cumulative concentration response curves to Carbachol (CCh; 1 nM–100 μM; Muscarinic agonist) and Potassium Chloride (KCl; 1–300 mM; Hyperpolarising agent) were

obtained in the basal tonus. The contractile response mediated by purinergic receptors was evaluated by the addition of 3 increasing concentrations of alpha, beta-methylene ATP (1, 3 and 10 μM) in a non-cumulative form, with an interval of 45 min between doses and tissues were washed three times during this period to avoid desensitization [10,31]. Data are shown as contraction mN/mg of tissue of n experiments, expressed as the mean values ± SEM.

2.7. Electrical-field stimulation (EFS)

Electrical field stimulation was applied in detrusor strips placed between two platinum ring electrodes connected to a grass S88 stimulator (Astro-Med Industrial Park, RI, USA). EFS was conducted at 80 V, 1-ms pulse width and trains of stimuli lasting 10s at varying frequencies (1–32 Hz) [32].

2.8. Polymerase chain reaction

Total ribonucleic acid (RNA) was extracted with Trizol Reagent (Gibco-BRL, Gaithersburg, MD, USA) from corpus cavernosum rat samples. RNA samples of 3 μg were incubated with 1 U deoxyribonuclease I (DNase-I) (Invitrogen, Rockville, MD) for 15 min at room temperature (RT) and EDTA was added to a final concentration of 2 mM to stop the reaction. The DNase-I enzyme was subsequently inactivated by incubation at 65 °C for 5 min. DNaseI-treated RNA samples were then reverse transcribed with Superscript III and Ribonuclease (RNaseOut) (Invitrogen Corporation, Carlsbad, CA) for 50 min at 50 °C, 15 min 70 °C. cDNA samples were quantified using a Nanodrop spectrophotometer (ND-1000; Nanodrop Technologies, Inc., Wilmington, DE). Synthetic oligonucleotide primers were designed to amplify cDNA for the genes encoding the muscarinic receptors (M_2 and M_3), metalloproteinase type-9 (MMP-9) and transforming growth factor - beta (TGF-β) and GAPDH (PrimerExpressTM; Applied Biosystems, Foster City, CA, USA). The primer sequences are listed in Table 1. All samples were assayed in a 12 μl volume containing 3 μl of 10 ng cDNA, 6 μl SYBR Green Master Mix Polymerase Chain Reaction and 3 μl of specific primers in a MicroAmp Optical 96-well reaction plate using the 7200 Sequence Detection System (Applied Biosystems, Foster City, CA). The threshold cycle (Ct) was defined as the point at which the fluorescence rises appreciably above the background fluorescence. The dissociation protocol was performed at the end of each run to check for nonspecific amplification. All samples were amplified in duplicate, and the mean of the threshold cycle was used for further calculations. The probe signal was normalized to an internal reference, and GAPDH was used as a reference gene; the fold increase was calculated by the conventional comparative CT (DDCt) method, as previously described in detail [33].

Table 1
Sequence and prime concentration for each primer pairs for the encoding muscarinic receptors (M_2 and M_3), metalloproteinase type-9 (MMP-9) and transforming growth factor - beta (TGF-β1).

Gene	Encoded protein	Primer sequence (5′-3′)	Primer concentration (nM)
Chrm2	M_2	F-TAGTTGGGTCGTCGGGTCAG	50
		R-CTTCACGATTTTGCGGGC	50
Chrm3	M_3	F-CCCACAGGCAGTTCTCGAA	150
		R-GAACCAGAAGTGACAGCGACC	150
Mmp9	MMP-9	F-AGGGAAGGCTCTGCTGATCA	300
		R-GACGTTGTGTGAGTTCCAGGG	300
Tgfb1	TGF-β1	F-CAGTGTTTCAGGCTAACCAAGAAA	150
		R-CCCGAATGTCTGACGTATTGAA	150
Gapdh	GAPDH	F-CCTGCCAAGTATGATGACATCAA	50
		F-AGCCCAGGATGCCCTTTAGT	50

F: Forward, R: Reverse.

2.9. Histological analysis

For histopathological analysis, specimens were fixed in 10% formol solution, embedded in paraffin blocks, and then subjected to sectioning for obtaining 4 μm slices. All the specimens were stained using hematoxylin and eosin (HE) for histomorphometric analysis by optical microscopy using computer-assisted image analysis. Briefly, a camera attached to the microscope captured the images selected on each slide. After capture and scanning, the images were evaluated by specific image analysis (NIS-Elements, Nikon®). The urothelial thickening and smooth muscle thickness was evaluated and this measurement was always made at the same magnification in a three representative fields of the sample. The average obtained after reading separate fields on the same slide in distinct field was considered for statistical analyses. Histopathological analysis was performed by two other researchers, without access to any other aspects of the study [34].

2.10. Drugs

Carbachol, alpha-beta metylene ATP, potassium chloride (Sigma Chem Co., St. Louis, MO, USA). Isoflurane, ketamine (UniãoQuímicaFarmacêutica Nacional S/A, Embu Guaçu, SP, Brazil) and xylazine (HertapeCalierSaúde Animal S/A, Juatuba, MG, Brazil). All reagents used were of analytical grade.

2.11. Statistical analysis

Data are expressed as mean ± SEM of n experiments. In the cumulative concentration-and frequency–response curves, data are expressed as means of the contraction in mN divided by the weight of the detrusor tissue ($mN{\cdot}mg^{-1}$) ± SEM of n experiments. The program Instat (GraphPad Software) was used for statistical analysis. For multiple comparisons of independent variables, the one-way ANOVA was used, followed by the *post hoc* Tukey test. Values of $p < 0.05$ were considered significant.

3. Results

3.1. The ACF model led to hypertrophy and cardiac dysfunction

The cardiac parameters are shown in Fig. 1 and the transthoracic echocardiography revealed that, after 4 and 12 weeks of ACF induction, the animals of the HF group demonstrated a significant increase in LV mass (Fig. 1A), fractional shortening of the LV posterior wall (Fig. 1E) and in the end LV diastolic volume (Fig. 1C), when compared to the Sham group. However, at 12 weeks the animals in the HF group presented a reduction of the ejection fraction (Fig. 1F) and an increase in the end LV systolic volume (Fig. 1B), when compared to Sham. In addition, when comparing HF groups at 4 and 12 weeks of fistula induction, there was a significant reduction in ejection fraction (Fig. 1F) and an increase in the final LV systolic volume (Fig. 1B), suggesting a progressive deterioration of the cardiac function of these animals.

3.2. HF rats displayed progressive urinary dysfunction

Fig. 2 shows a representative tracing of cystometry in Sham and HF (4 and 12 weeks) rats. The pattern of urination of Sham rats showed rare involuntary contractions (panel A), whereas HF rats exhibited an irregular pattern of micturition, with uninhibited contractions along the trajectory, both at 4 and 12 weeks (panel B and C, respect). The analysis of the cystometric parameters showed that, after 4 weeks of ACF induction, HF rats presented a significant increase in voiding pressure (VP) (Fig. 3B), threshold pressure (TP) (Fig. 3C), associated with a significant decrease in bladder capacity, compared to Sham group (Fig. 3D). After 12 weeks, HF rats showed a significant increase in VP (Fig. 3B) and in the frequency of non-voiding contractions (NVC)

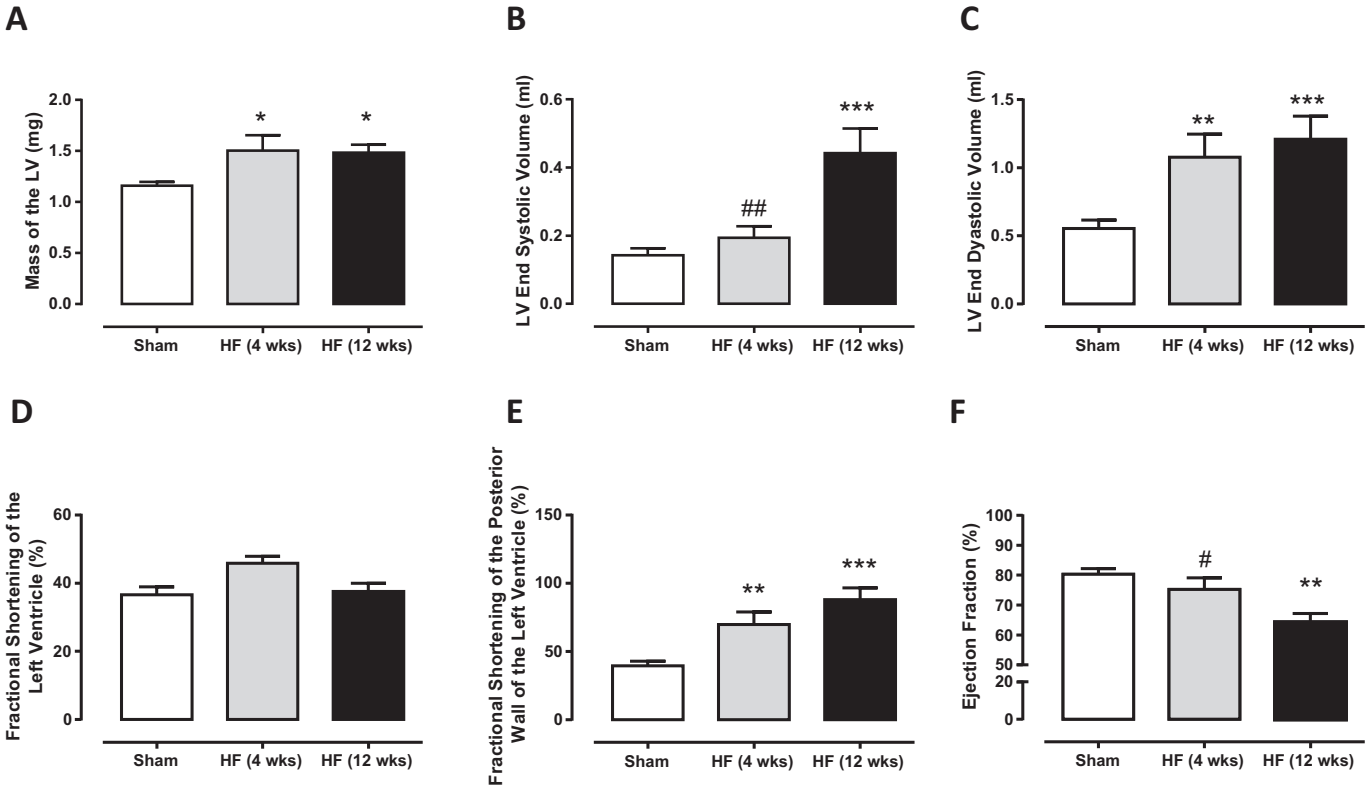

Fig. 1. Impact of the ACF model on animals cardiac function.
Echocardiographic exploration of cardiac function in sham and heart failure (HF; 4 and 12 weeks) animals. Measurements of left ventricular (LV) mass (panel A), LV end systolic volume (panel B), LV end diastolic (panel C), fractional shortening of LV (panel D), fractional shortening of the posterior wall of LV (panel E) and ejection fraction (panel F). Data are mean ± SEM of 5 experiments. *$p < 0.05$; **$p < 0.01$; **$p < 0.001$ compared to sham group. $^{\#\#}p < 0.01$ compared to HF group.

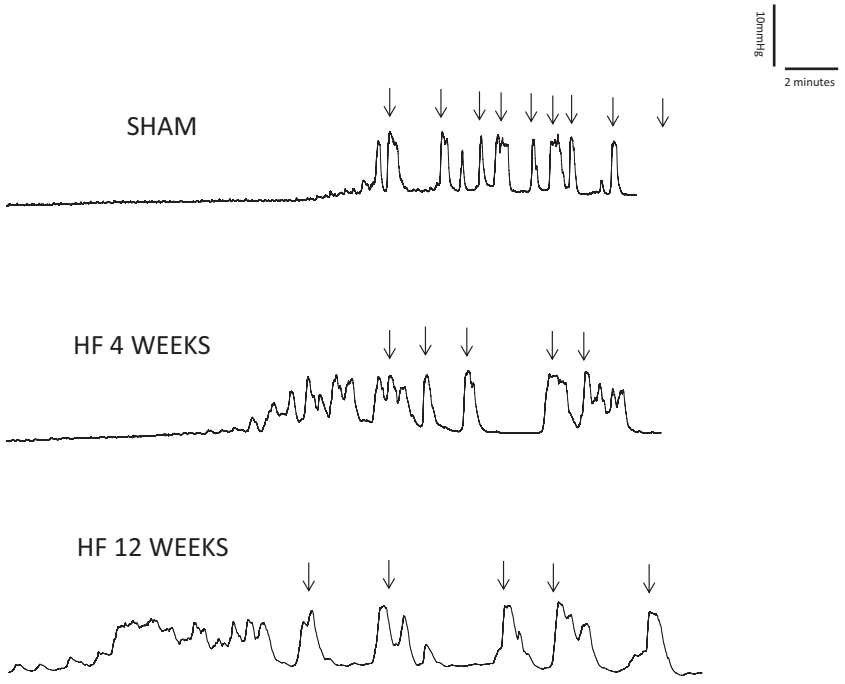

Fig. 2. Cystometric tracings.
Representative traces of cystometry from Sham and heart failure (HF; 4 and 12 weeks) groups. Sham (panel A) and HF (panel B and C, respect.). The tracings represent 30 min of experimental procedure and the arrows indicate the presence of urination.

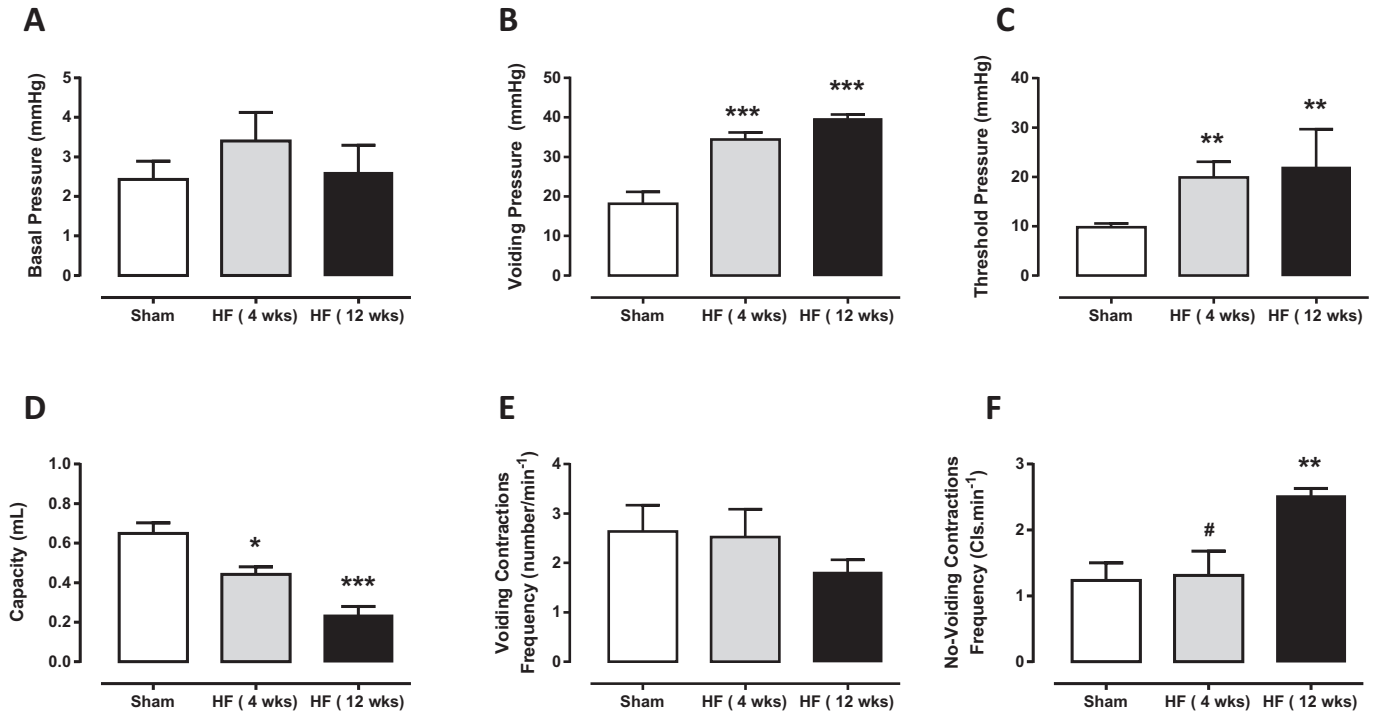

Fig. 3. Effect of HF on urinary function *in vivo*.
Cystometric parameters of animals Sham (n = 12) and heart failure (HF) 4 (n = 5) and 12 (n = 5) weeks. Were measured at basal pressure (BP; panel A), voiding pressure (VP; panel B), threshold pressure (TP; panel C), capacity (CP; panel D), voiding contractions frequency (VC; panel E) and non-voiding contractions frequency (NVC; panel F). Data are mean ± SEM of n experiments. *p < 0.05; **p < 0.01; ***p < 0.001compared to sham group. #p < 0.05 compared to HF group.

(Fig. 3F), associated with a decrease in bladder capacity, when compared to the Sham group (Fig. 3D). In addition, when comparing HF groups at 4 and 12 weeks of ACF induction, a significant increase in NVC was observed over the weeks (Fig. 3F), showing a progression of symptoms associated with the stage of the disorder.

3.3. HF rats exhibited contractile mechanism dysfunction

The cumulative addition of the non-selective muscarinic receptor agonist carbachol (CCh) caused a concentration-dependent contraction of the DSM in Sham and HF groups (4 and 12 weeks). The potency (pEC_{50}) of CCh was not significantly altered in the HF groups compared to the respective Sham groups (Table 2). However, the maximum contractile response to CCh (Emax) in DSM was significantly elevated in HF 4 and 12 weeks groups when compared to Sham group (Fig. 4A).

Similarly, the non-cumulative addition of the P2X receptor agonist (alpha, beta-methylene ATP; ATP) promoted at all concentrations (1, 3 and 10 μM) a significant increase in the contractile response of DSM in HF groups compared to Sham group, when compared to Sham group (Fig. 4C).

Receptor-independent contractile effects were assessed by constructing concentration-response curves to the hyperpolarising agent potassium chloride (KCl) in the DSM of rats under basal tonus. The potency (pEC_{50}) of KCl was not significantly altered in HF groups, compared to Sham. However, the results showed a significant increase in the maximum response (Emax) of the DSM in HF groups compared to Sham group (Fig. 4B). The potency (pEC_{50}) and maximal responses (Emax) values are represented in Table 2.

Table 2
Potency (pEC_{50}) and maximal responses (E_{max}) values obtained from concentration–response curves in detrusor muscle strips from Sham and HF rats.

Groups	Carbachol (CCh)		Potassium Chloride (KCl)	
	pEC_{50}	E_{max}	pEC_{50}	E_{max}
Sham	5.60 ± 0.06	0.91 ± 0.05	0.97 ± 0.17	0.76 ± 0.06
HF 4 weeks	5.73 ± 0.08	1.25 ± 0.10*,#	1.09 ± 0.09	1.03 ± 0.07*,#
HF 12 weeks	5.69 ± 0.04	1.54 ± 0.07**	1.06 ± 0.04	1.30 ± 0.07***

Data represent the mean ± S.E.M. of 6–9 experiments. *p < 0.05, **p < 0.01, ***p < 0.001 compared with Sham group; #p < 0.05 compared with HF 12 weeks group.

3.4. The response to electrical field stimulation was increased in HF rats

Electrical field stimulation (EFS) induces depolarization of cholinergic and non-adrenergic non-cholinergic neurons to induce contractions of the DSM under basal tonus. Construction of frequency-response curves in the DSM showed a frequency-dependent contraction in Sham and HF groups. However, the magnitude of the contraction elicited by EFS at all frequencies was significantly higher in the DSM of the HF group at 12 weeks, when compared to the respective Sham group or HF group at 4 weeks (Fig. 4D).

3.5. HF rats displayed increased expression of mRNA for the M_2 and M_3 receptors, MMP-9 and TGF-beta in the DSM

The evaluation of the urinary bladders of HF group at 12 weeks showed a significant increase in the gene expression of muscarinic M2 and M3 receptors mRNA, when compared to Sham and HF at 4 weeks. Expression of MMP-9 and TGF-beta mRNA were also significantly increased in the urinary bladder of the 12-week HF animals, when compared to the 4 week Sham and HF groups (Fig. 5).

3.6. HF rats showed morphological changes in the urinary bladder

Morphological analysis of the urinary bladder showed significant structural changes, which were observed as a significant thickening of the urothelial layer in HF at 4 and 12 weeks, compared to the age-

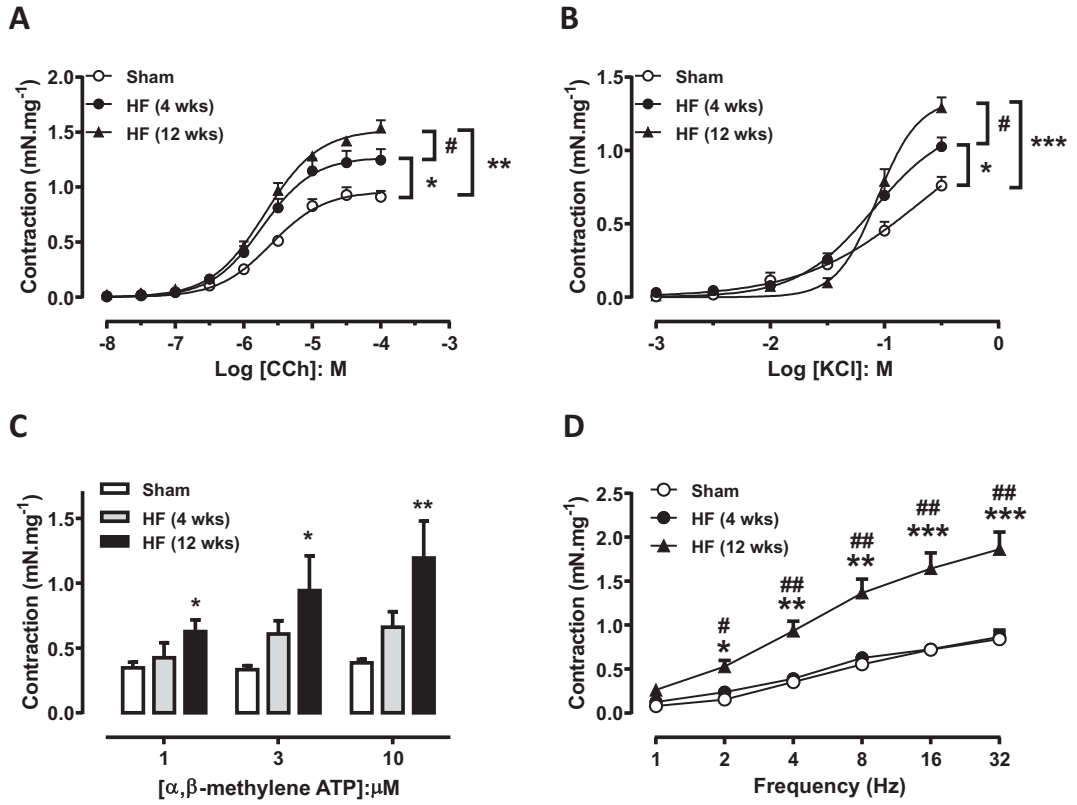

Fig. 4. Hyperactivation of contractile mechanisms.
Concentration response curves to carbachol (CCh; panel A), potassium chloride (KCl; panel B), α,β-methylene ATP (ATP; panel C) in detrusor muscle strips from Sham (n = 9, 8 and 8, respect.) and heart failure (HF) 4 (n = 6, 4 and 4, respect.) and 12 (n = 6, 4 and 5, respect.) weeks. Frequency response curve to electrical field stimulation (EFS; 1-32 Hz; panel D) in detrusor muscle strips from Sham (n = 11) and heart failure (HF) 4 (n = 5) and 12 (n = 6) weeks. The contraction was calculated as the absolute value in mN divided by the individual weight of each strip ($mN \cdot mg^{-1}$). Data are mean ± SEM of n experiments. *p < 0.05; **p < 0.01; ***p < 0.001compared to Sham group. #p < 0.05; ##p < 0.01 compared to HF group.

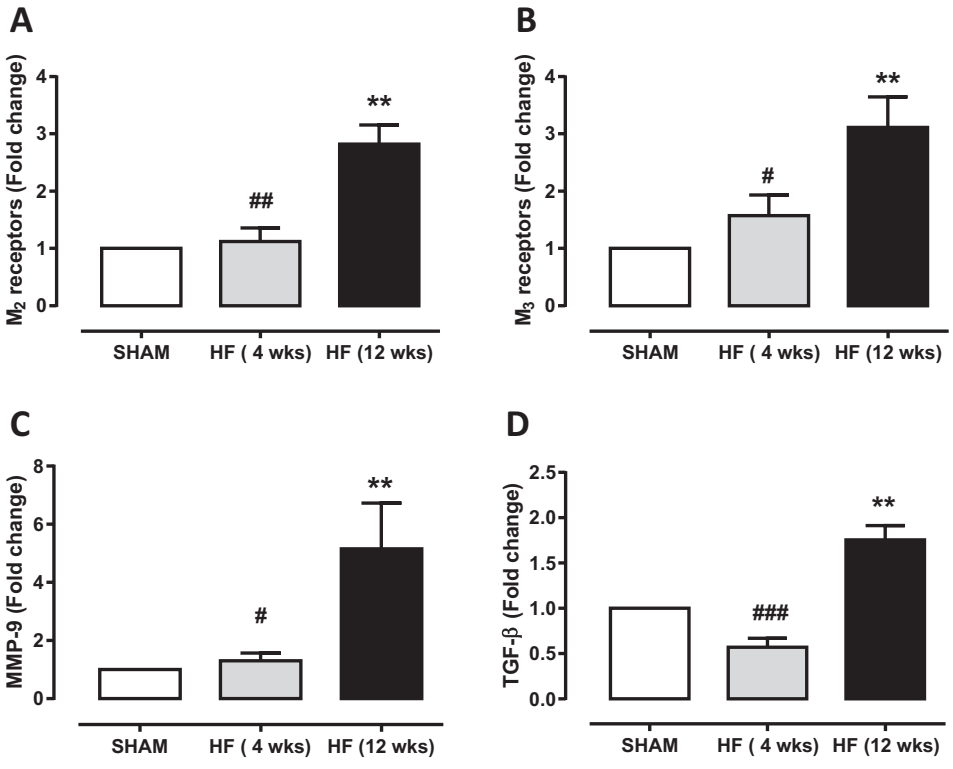

Fig. 5. mRNA expression of muscarinic M2 and M3 receptors (panel A and B respect.), matrix metallopeptidase 9 (MMP9; panel C) and transforming growth factor beta (TGF-beta; panel D) in the homogenates of the bladder from sham and heart failure (HF; 4 and 12 weeks) rats.
The mRNA expression level of each gene was normalized by GAPDH expression. Data represent the means ± SEM of 4–6 experiments in each group. **p < 0.01 compared to Sham group. #p < 0.05; ##p < 0.01; ###p < 0.001 compared to HF group (12 wks).

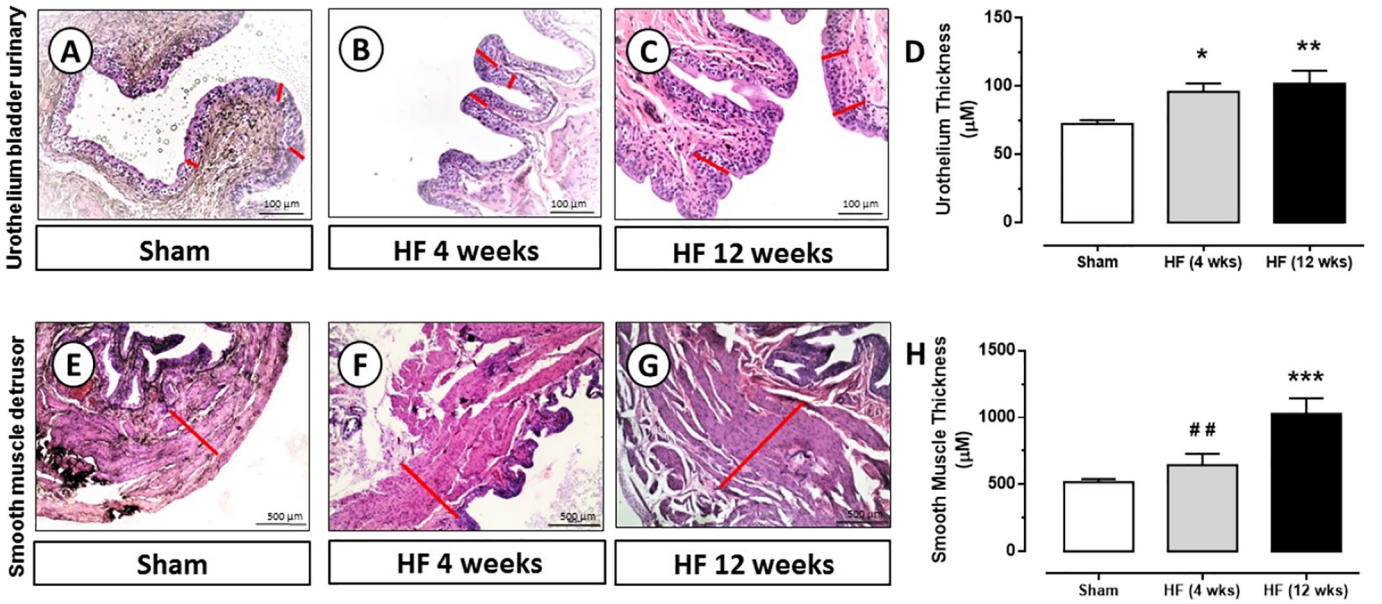

Fig. 6. Structural impairment of urothelium and detrusor musculature.
Measurements of urothelium thickness (panel D) and smooth detrusor thickness (panel H) in the Sham (n = 6) and heart failure (HF) 4 (n = 2) and 12 (n = 3) weeks. Data are mean ± SEM of n experiments. *p < 0.05; **p < 0.01 compared to Sham group. Images representative of the histomorphometric analysis of the urothelium (panel A to C) and smooth detrusor muscle (panel E to G) after staining with hematoxylin and eosin in the Sham and heart failure (HF; 4 and 12 weeks) groups. Note the urothelial thickening (4 and 12 weeks) and the detrusor muscle layer thickness (12 weeks) in the HF when compared to Sham group (scale bar: 100 µM).

matched Sham group (Fig. 6A to D). In addition, HF at 12 weeks also presented a significant increase in the thickness of DSM, when compared to the age-matched Shamor HF at 4 weeks (Fig. 6E to H).

4. Discussion

In the present work, the surgical model of ACF caused changes in the hemodynamic flow which were accompanied by the development of OAB and alterations in the reactivity and structure of the DSM, revealed by changes in the cystometry parameters, increased receptor - dependent and - independent contractile responses and thickening of the urothelium and DSM layers of the bladder.

Several experimental models of HF have been created over recent years with the purpose of helping to understand the mechanisms related to their development and their complications. These include aortic banding, coronary artery ligation, ACF, and spontaneously hypertensive animals [35–37]. The ACF model has been widely used today and consists of the creation of a fistula below the renal arteries, resulting in a decrease in mean arterial pressure and an overload of venous volume to the right heart chambers. Such hemodynamic changes lead to the activation of numerous compensatory neurohumoral mechanisms and cardiac manifestations, such as decreased ejection fraction, hypertrophy and cardiac remodeling [24].

Our results demonstrate that, after 4 and 12 weeks of ACF induction, animals showed an increase in total cardiac mass, suggesting that the vascular changes resulting from the model had a significant cardiac overload and consequent hypertrophy as early as the first weeks after fistula induction and were progressive until the 12th week. In addition to the hypertrophy, our animals also presented cardiac function impairment at 4 and 12 weeks, since there was a progressive decrease in the ejection fraction and increase in left ventricular end systolic and diastolic volumes, demonstrating that the ACF model led to structural and functional alterations that characterize HF. Our findings corroborate previous studies reporting similar cardiac abnormalities following the induction of ACF in rats [25,29,38].

The development of LUTS, such as urinary urgency, urinary incontinence and OAB, may represent a burden to the quality of life of the patient in many cardiovascular diseases. Studies have shown an intimate relationship between HF and LUTS [6,8] and it is believed that several mechanisms involved in the pathophysiology of HF may contribute to the progression of LUTS. Among these mechanisms, endothelial dysfunction, arterial insufficiency, increased levels of vasoconstricting agents, autonomic hyperactivity and pharmacological treatment may cause autonomic dysfunction and important molecular alterations in the signaling pathways that control the smooth muscle tone. Furthermore, patients with HF exhibit worsened renal function and tubular damage [39,40] which could increase the level of toxic substances accumulated in the urine and stored in the bladder and might also contribute to its functional impairment. In addition, clinical and experimental studies indicate that chronic pelvic ischemia during the voiding cycle may result in reduced NO bioavailability, leading to endothelial dysfunction and increased formation of reactive oxygen species in the bladder [41–43]. Furthermore, enhanced activity of muscarinic receptors causes structural damage to the DSM and neurodegeneration and impairs urinary function in both animals and humans [44–46].

Therefore, since LUTS may occur in HF patients, herein we evaluated the urinary function of rats submitted to ACF model of HF. Initially, cystometric parameters (*in vivo*) were evaluated in anesthetized animals. Continuous infusion of saline into the bladder demonstrated reduced bladder capacity in the HF group at 4 weeks, with consequent elevation of urination contractions and threshold pressure during the bladder filling phase. Similarly, the HF group exhibited the same pattern of decreased capacity and increased threshold pressure at 12 weeks; however, a higher number of involuntary contractions was also observed, characterizing OAB. Taken together, these data suggest that the hemodynamic changes imposed by the ACF model resulted in impaired urinary function during the weeks after HF induction. In addition, the deterioration of urinary function was progressive and may be associated with the evolution of HF. Micturition dysfunction has been observed in experimental models of chronic ischemia of the urinary bladder [21,47,48], but never in the ACF model. To the best of our knowledge, this is the first study showing that HF is associated with the impairment of urinary function, independently of treatments

frequently prescribed for patients with HF. Although LUTS are not one of the first issues for treatment in HF patients, theses urinary symptoms are 2.9 times more prevalent in Class III- or Class IV-functional HF patients, compared with Class I or Class II [6,7], providing evidence that urinary function impairment may follow the progression of the disease [6].

The understanding of pathophysiological alterations leading to the development of OAB associated with HF is necessary and may be useful for the development of effective OAB therapies. Thus, in this study we also evaluated the contractile response mechanisms in the DSM. The urinary cycle depends on a well-coordinated action between the sympathetic and parasympathetic systems, which act releasing neurotransmitters and favor the mechanisms of relaxation and contraction, respectively, in the DSM [49]. The main parasympathetic neurotransmitter is acetylcholine (ACh), which stimulates muscarinic receptors to cause contraction of the DSM. ATP is stored and released together with Ach and promotes contractility through the activation of purinergic receptors [50,51]. Studies indicate the presence of ACh synthesizing enzymes in the urothelium, confirming a basal release of this neurotransmitter during homeostatic situations [52]. However, some pathological conditions may result in chemical changes or stretching of the DSM, increasing the release of Ach and resulting in muscarinic receptor sensitization and consequent release of ATP, leading to afferent hyperactivity and triggering the symptoms of OAB [53]. In the *in vitro* evaluation of the contractile response mediated by muscarinic and purinergic agonists our data showed an increase in contractility mediated by both mediators in HF groups. Similarly, an increase in the contractile response was observed to be mediated by EFS, which may be the consequence of increased release of ACh and ATP from neuronal sources, although activation of other NANC neurons by EFS was not addressed in this study, and their involvement cannot be discarded. Corroborating the hyperactivity observed in the *in vitro* analysis, our data showed a significant increase in the gene expression of M2 muscarinic receptors, responsible for one of the main contractile routes in DSM and mediating the contraction of DSM triggered by acetylcholine derived from the stimulation of the parasympathetic nervous system [50].

The increase in the contractile response, mediated by purinergic receptors, may be associated with TGF-beta gene expression, which was elevated in the HF group at 12 weeks. Recent studies have shown that, in pathological conditions, TGF-beta-mediated signaling in DSM may contribute significantly to the picture of voiding dysfunction, because it stimulates the release of ATP by the urothelium through mechanisms of vesicular exocytosis and contributes to the hyperexcitability of afferent neurons, mediated by the purinergic system [54,55]. TGF-beta has also been implicated as playing an important role in pathological remodeling of the urinary bladder wall, increasing the production of type I and II collagen, inducing hypertrophy and inhibiting cellular proliferation in the bladder [54,56].

In addition, another mechanism that may be involved in detrusor over activity is the activation of Cav1.2 calcium channels. It is known that M3 muscarinic receptors are capable of promoting calcium release through the activation of the inositol-1,4,5-trisphosphate (IP 3) receptor, inducing contractions that depend on the entry of calcium into the Cav1.2 channels [31]. The elevation of extracellular potassium levels is able to activate these channels and induce conformable responses in the DSM. Some studies have reported the importance of Cav1.2 channels in the development of DSM hyperactivity in experimental models of cardiovascular diseases [57]. Our results demonstrate that KCl-mediated contractility was exacerbated in the HF group at 4 and 12 weeks, which might be a consequence of the chronic pelvic ischemia imposed by HF, leading to hyperactivity of the muscarinic receptors and consequently of the Cav1.2 channels.

The hyperactivation of contractile mechanisms mediated by EFS and KCl corroborates our initial hypothesis that HF leads to DSM hyperactivity and provides a basis for the major changes observed *in vivo*, such as decreased bladder capacity, increased threshold pressure and involuntary contractions. In association with functional impairment, histomorphometric analysis showed thickening of the urothelial layer and DSM as early on as during the first 4 weeks after HF induction, with progressive worsening in the HF group at 12 weeks. Studies in experimental models of transitional cell carcinoma have demonstrated a strong association between increased MMP9 expression and progression of invasive muscle disease, since the secretion of MMP9 by tumor cells stimulates the invasion of adjacent tissues and tumor proliferation through degradation of extracellular matrix components [58,59]. In HF, induced by the ACF model, there are no studies correlating the expression of MMP9 and the possible urinary complications developed by the animals. In our study, an increased expression of MMP9 was observed, accompanied by a progressive structural impairment of the urothelium and DSM in the HF groups, suggesting a participation of MMP9 in the evolution of structural changes in non-oncological urinary disorders.

In summary, our study demonstrated that the hemodynamic changes promoted by the ACF model led to the development of cardiac dysfunction and progressive micturition dysfunction over time. Our findings also indicated that OAB was accompanied by increased contractile responses to CCh, KCl, ATP and EFS in DSM as well as extracellular matrix remodeling in the urinary bladder. Moreover, the model of ACF in rats may be a useful tool to evaluate the structural and molecular alterations of OAB associated with HF.

Credit author statement

AGM, SRF, FBMP and MAC designed the experiment and analysed data. KK performed cardiac analysis. AGM, SRF, DRA and JSC performed the *in vitro* and *in vivo* experiments. FPCF and MAC performed molecular analysis. SPT, RT and DGP performed histological analysis. MAC co-ordinated the experiments. AGM, FBMP and MAC drafted the article. All authors have approved the final version of the manuscript submitted for publication and agree to be accountable for all aspects of the work.

Grants

This study was supported by grant from FAPESP (2011/21095-4).

Conflicts of interest

The authors declare that they have no competing interest with the contents of this article.

Author contributions

AGM, SRF, FBMP and MAC designed the experiment and analysed data. KK performed cardiac analysis. AGM, SRF, DRA and JSC performed the *in vitro* and *in vivo* experiments. FPCF and MAC performed molecular analysis. SPT, RT and DGP performed histological analysis. MAC co-ordinated the experiments. AGM, FBMP and MAC drafted the article. All authors have approved the final version of the manuscript submitted for publication and agree to be accountable for all aspects of the work.

References

[1] E. Crimi, L. Ignarro, F. Cacciatore, C. Napoli, Mechanisms by which exercise training benefits patients with heart failure, Nat. Rev. Cardiol. 6 (2009) 292–300, https://doi.org/10.1038/nrcardio.2009.8.

[2] B. Xu, H. Li, Brain mechanisms of sympathetic activation in heart failure: roles of the renin-angiotensin system, nitric oxide and pro-inflammatory cytokines (review), Mol. Med. Rep. 12 (2015) 823–829, https://doi.org/10.3892/mmr.2015.4434.

[3] P. Heidenreich, N. Albert, L. Allen, D. Bluemke, J. Butler, G. Fonarow, J. Ikonomidis, O. Khavjou, M. Konstam, T. Maddox, G. Nichol, M. Pham, I. Pina,

J. Trogdon, Forecasting the impact of heart failure in the United States: a policy statement from the american heart association, Circ. Heart Fail. 6 (2013) 606–619, https://doi.org/10.1161/HHF.0b013e318291329a.
[4] A. Go, et al., Heart disease and stroke statistics—2014 update: a report from the American Heart Association, Circulation 129 (2013) e28–e292, https://doi.org/10.1161/01.cir.0000441139.02102.80.
[5] T. Griebling, Re: high classification of chronic heart failure increases risk of overactive bladder syndrome and lower urinary tract symptoms, J. Urol. 189 (2013) 1821, https://doi.org/10.1016/j.juro.2013.02.054.
[6] M. Palmer, S. Hardin, C. Behrend, S. Collins, C. Madigan, J. Carlson, Urinary incontinence and overactive bladder in patients with heart failure, J. Urol. 182 (2009) 196–202, https://doi.org/10.1016/j.juro.2009.02.115.
[7] C. Tannenbaum, K. Johnell, Managing therapeutic competition in patients with heart failure, lower urinary tract symptoms and incontinence, Drugs Aging 31 (2014) 93–101, https://doi.org/10.1007/s40266-013-0145-1.
[8] A.S. Bierman, Coexisting illness and heart disease among elderly medicare managed care enrollees, Health Care Financ. Rev. 25 (2004) 105–117 (PMC4194893).
[9] P. Abrams, L. Cardozo, M. Fall, D. Griffiths, P. Rosier, U. Ulmsten, P. van Kerrebroeck, A. Victor, A. Wein, The standardisation of terminology of lower urinary tract function: report from the standardisation sub-committee of the international continence society, Am. J. Obstet. Gynecol. 187 (2002) 116–126 (PMID: 12114899).
[10] M. Claudino, L. Leiria, F. da Silva, E. Alexandre, A. Renno, F. Mónica, G. de Nucci, K. Fertrin, E. Antunes, F. Costa, C. Franco-Penteado, Urinary bladder dysfunction in transgenic sickle cell disease mice, PLoS One 10 (2015) e0133996, , https://doi.org/10.1371/journal.pone.0133996.
[11] S. Bonilla-Becerra, M. de Oliveira, F. Calmasini, J. Rojas-Moscoso, A. Zanesco, E. Antunes, Micturition dysfunction in four-month old ovariectomized rats: effects of testosterone replacement, Life Sci. 179 (2017) 120–129, https://doi.org/10.1016/j.lfs.2017.05.006.
[12] K. Andersson, Urinary bladder contraction and relaxation: physiology and pathophysiology, Physiol. Rev. 84 (2004) 935–986, https://doi.org/10.1152/physrev.00038.2003.
[13] M. Michel, W. Vrydag, α1-, α2- and β-Adrenoceptors in the urinary bladder, urethra and prostate, Br. J. Pharmacol. 147 (2006) S88–S119, https://doi.org/10.1038/sj.bjp.0706619.
[14] K. Andersson, A.J. Wein, Pharmacology of the lower urinary tract: basis for current and future treatments of urinary incontinence, Pharmacol. Rev. 56 (2004) 581–631, https://doi.org/10.1124/pr.56.4.4.
[15] G. Burnstock, Therapeutic potential of purinergic signalling for diseases of the urinary tract, BJU Int. 107 (2011) 192–204, https://doi.org/10.1016/j.bcp.2017.07.016.
[16] X.D. Liu, J.H. Chen, H.Y. Li, H. Li, S. Yin, Expression of type 3 acid sensitive ion channels in bladder of oab rat model, Sichuan Da Xue Xue Bao Yi Xue Ban 47 (2016) 174–179 (PMID: 27263289).
[17] B. Parsons, M. Drake, Animal models in overactive bladder research, HandbExpPharmacol 202 (2011) 15–43, https://doi.org/10.1007/978-3-642-16499-6_2.
[18] M. Drake, A. Kanai, D. Bijos, Y. Ikeda, I. Zabbarova, B. Vahabi, C. Fry, The potential role of unregulated autonomous bladder micromotions in urinary storage and voiding dysfunction; overactive bladder and detrusor underactivity, BJU Int. 119 (2017) 22–29, https://doi.org/10.1111/bju.13598.
[19] Y. Matsukawa, S. Takai, Y. Funahashi, T. Yamamoto, M. Gotoh, Urodynamic evaluation of the efficacy of mirabegron on storage and voiding functions in women with overactive bladder, Urology 85 (2015) 786–790, https://doi.org/10.1016/j.urology.2015.01.002.
[20] A. Apostolo, C. Vignati, D. Brusoni, G. Cattadori, M. Contini, F. Veglia, D. Magrì, P. Palermo, C. Tedesco, E. Doria, C. Fiorentini, P. Montorsi, P. Agostoni, Original research—erectile dysfunction: erectile dysfunction in heart failure: correlation with severity, exercise performance, comorbidities, and heart failure treatment, J. Sex. Med. 6 (2009) 2795–2805, https://doi.org/10.1111/j.1743-6109.2009.01416.x.
[21] K. Andersson, D. Boedtkjer, A. Forman, The link between vascular dysfunction, bladder ischemia, and aging bladder dysfunction, Ther. Adv. Urol. 9 (2017) 11–27, https://doi.org/10.1177/1756287216675778.
[22] C. Asche, J. Kim, A. Kulkarni, P. Chakravarti, K. Andersson, Presence of central nervous system, cardiovascular and overall co-morbidity burden in patients with overactive bladder disorder in a real-world setting, BJU Int. 109 (2012) 572–580, https://doi.org/10.1111/j.1464-410X.2011.10436.x.
[23] I. Milsom, P. Abrams, L. Cardozo, R. Roberts, J. Thüroff, A. Wein, How widespread are the symptoms of an overactive bladder and how are they managed? A population-based prevalence study, BJU Int. 87 (2001) 760–766 (PMID: 11412210).
[24] Z. Abassi, I. Goltsman, T. Karram, J. Winaver, A. Hoffman, Aortocaval fistula in rat: a unique model of volume-overload congestive heart failure and cardiac hypertrophy, J. Biomed. Biotechnol. 2011 (2011) 1–13, https://doi.org/10.1155/2011/729497.
[25] K. Nagalla, M. Gole, M. Claudino, J. Gardner, D. Murray, Alteration in myocardial prostaglandin D synthase expression in pressure overload-induced left ventricular remodeling in rats, Exp. Biol. Med. 237 (2012) 24–30, https://doi.org/10.1258/ebm.2011.011180.
[26] K. Azadzoi, Z. Radisavljevic, T. Golabek, S. Yalla, M. Siroky, Oxidative modification of mitochondrial integrity and nerve fiber density in the ischemic overactive bladder, J. Urol. 183 (2010) 362–369, https://doi.org/10.1016/j.juro.2009.08.103.
[27] J. Greenland, A. Brading, The effect of bladder outflow obstruction on detrusor blood flow changes during the voiding cycle in conscious pigs, J. Urol. 165 (2001) 245–248, https://doi.org/10.1097/00005392-200101000-00072.
[28] J. Gardner, D. Murray, T. Voloshenyuk, G. Brower, J. Bradley, J. Janicki, Estrogen attenuates chronic volume overload induced structural and functional remodeling in male rat hearts, AJP: Heart Circ. Physiol. 298 (2009) H497–H504, https://doi.org/10.1152/ajpheart.00336.2009.
[29] F.H. Silva, F.J.R. Veiga, A.G. Mora, R.S. Heck, C.C. De Oliveira, A. Gambero, C.F. Franco-Penteado, E. Antunes, J.D. Gardner, F.B.M. Priviero, M.A. Claudino, A novel experimental model of erectile dysfunction in rats with heart failure using volume overload, PLoS One 12 (11) (2017) e0187083, , https://doi.org/10.1371/journal.pone.0187083.
[30] F. Rodrigues, R. Lopes, R. Fais, L. de Oliveira, C. Prado, R. Tostes, F. Carneiro, Erectile dysfunction in heart failure rats is associated with increased neurogenic contractions in cavernous tissue and internal pudendal artery, Life Sci. 145 (2016) 9–18, https://doi.org/10.1016/j.lfs.2015.12.005.
[31] A. Ramos-Filho, F. Mónica, C. Franco-Penteado, J. Rojas-Moscoso, F. Báu, A. Schenka, G. De Nucci, E. Antunes, Characterization of the urinary bladder dysfunction in renovascular hypertensive rats, Neurourol. Urodyn. 30 (2011) 1392–1402, https://doi.org/10.1002/nau.21074.
[32] M. Claudino, C. Franco-Penteado, F. Priviero, E. Camargo, S. Teixeira, M. Muscará, G. De Nucci, A. Zanesco, E. Antunes, Upregulation of gp91phox subunit of nad(p)h oxidase contributes to erectile dysfunction caused by long-term nitric oxide inhibition in rats: reversion by regular physical training, Urology 75 (2010) 961–967, https://doi.org/10.1016/j.urology.2009.05.098.
[33] J. Vandesompele, K. De Preter, F. Pattyn, B. Poppe, N. Van Roy, A. De Paepe, F. Speleman, Accurate normalization of real-time quantitative RT-PCR data by geometric averaging of multiple internal control genes, Genome Biol. 7 (2002) (Research0034. PMID: 12184808).
[34] D. Campos Peseto, E. Carmona, K. Silva, F. Guedes, F. Hummel Filho, N. Martinez, J. Pereira, T. Rocha, D. Priolli, Effects of tretinoin on wound healing in aged skin, Wound Repair Regen. 24 (2016) 411–417, https://doi.org/10.1111/wrr.12417.
[35] R. Garcia, S. Diebold, Simple, rapid, and effective method of producing aortocaval shunts in the rat, Cardiovasc. Res. 24 (1990) 430–432 (PMID: 2142618).
[36] T. Karram, A. Hoffman, B. Bishara, S. Brodsky, E. Golomb, J. Winaver, Z. Abassi, Induction of cardiac hypertrophy by a controlled reproducible suturelessaortocaval shunt in the mouse, J. Investig. Surg. 18 (2005) 325–334, https://doi.org/10.1080/08941930500328839.
[37] J. Winaver, A. Hoffman, J.C. Burnett Jr., A. Haramati, Hormonal determinants of sodium excretion in rats with experimental high-output heart failure, Am. J. Phys. 254 (1988) R776–R784, https://doi.org/10.1152/ajpregu.1988.254.5.R776.
[38] K. Wilson, A. Guggilam, T. West, X. Zhang, A. Trask, M. Cismowski, P. de Tombe, S. Sadayappan, P. Lucchesi, Effects of a myofilament calcium sensitizer on left ventricular systolic and diastolic function in rats with volume overload heart failure, AJP: Heart Circ. Physiol. 307 (2014) H1605–H1617, https://doi.org/10.1152/ajpheart.00423.2014.
[39] K. Damman, S. Masson, H.L. Hillege, A.P. Maggioni, A.A. Voors, C. Opasich, D.J. van Veldhuisen, L. Montagna, F. Cosmi, G. Tognoni, L. Tavazzi, R. Latini, Clinical outcome of renal tubular damage in chronic heart failure, Eur. Heart J. 32 (21) (2011) 2705–2712, https://doi.org/10.1093/eurheartj/ehr190.
[40] Y. Okubo, A. Sairaku, N. Morishima, H. Ogi, T. Matsumoto, H. Kinoshita, Y. Kihara, Increased urinary liver-type fatty acid-binding protein level predicts worsening renal function in patients with acute heart failure, J. Card. Fail. S1071-9164 (18) (2018) 30276–30278, https://doi.org/10.1016/j.cardfail.2018.07.003.
[41] M. Ho, N. Bhatia, O. Khorram, Physiologic role of nitric oxide and nitric oxide synthase in female lower urinary tract, Curr. Opin. Obstet. Gynecol. 16 (2004) 423–429 (PMID: 15353953).
[42] J. Hall, Obesity hypertension: role of leptin and sympathetic nervous system, Am. J. Hypertens. 14 (2001) S103–S115 (PMID: 11411745).
[43] K. Hubeaux, X. Deffieux, S. Ismael, P. Raibaut, G. Amarenco, Autonomic nervous system activity during bladder filling assessed by heart rate variability analysis in women with idiopathic overactive bladder syndrome or stress urinary incontinence, J. Urol. 178 (2007) 2483–2487, https://doi.org/10.1016/j.juro.2007.08.036.
[44] K. Andersson, A. Arner, Urinary bladder contraction and relaxation: physiology and pathophysiology, Physiol. Rev. 84 (2004) 935–986, https://doi.org/10.1152/physrev.00038.2003.
[45] F. Báu, F. Mónica, F. Priviero, L. Baldissera, G. de Nucci, E. Antunes, Evaluation of the relaxant effect of the nitric oxide-independent soluble guanylyl cyclase stimulator BAY 41-2272 in isolated detrusor smooth muscle, Eur. J. Pharmacol. 637 (2010) 171–177, https://doi.org/10.1016/j.ejphar.2010.04.008.
[46] S. Propping, M. Roedel, M. Wirth, U. Ravens, Pharmacological modulation of mucosa-related impairment of beta-adrenoceptor-mediated relaxation in human detrusor, Urol. Int. 95 (2015) 300–308, https://doi.org/10.1159/000431260.
[47] M. Nomiya, K. Sagawa, J. Yazaki, N. Takahashi, N. Kushida, N. Haga, K. Aikawa, T. Matsui, M. Oka, T. Fukui, K. Andersson, O. Yamaguchi, Increased bladder activity is associated with elevated oxidative stress markers and proinflammatory cytokines in a rat model of atherosclerosis-induced chronic bladder ischemia, Neurourol. Urodyn. 31 (2012) 185–189, https://doi.org/10.1002/nau.21191.
[48] A. Wein, Re: protective effect of a β3-adrenoceptor agonist on bladder function in a rat model of chronic bladder ischemia, J. Urol. 193 (2015) 2148–2149, https://doi.org/10.1016/j.juro.2015.03.061.
[49] E. Frazier, S. Peters, A. Braverman, M. Ruggieri, M. Michel, Signal transduction underlying the control of urinary bladder smooth muscle tone by muscarinic receptors and β-adrenoceptors, Naunyn Schmiedeberg's Arch. Pharmacol. 377 (2007) 449–462, https://doi.org/10.1007/s00210-007-0208-0.
[50] G. Burnstock, M. Williams, P2 purinergic receptors: modulation of cell function and therapeutic potential, J. Pharmacol. Exp. Ther. 295 (2000) 862–869 (PMID: 11082418).
[51] A.P. Ford, D.A. Cockayne, ATP and P2X purinoceptors in urinary tract disorders,

HandbExpPharmacol 202 (2011) 485–526, https://doi.org/10.1007/978-3-642-16499-6_22.
[52] M. Yoshida, A. Inadome, Y. Maeda, Y. Satoji, K. Masunaga, Y. Sugiyama, S. Murakami, Non-neuronal cholinergic system in human bladder urothelium, Urology 67 (2006) 425–430, https://doi.org/10.1016/j.urology.2005.08.014.
[53] S. Cellek, N. Cameron, M. Cotter, C. Fry, D. Ilo, Microvascular dysfunction and efficacy of PDE5 inhibitors in BPH–LUTS, Nat. Rev. Urology 11 (2014) 231–241, https://doi.org/10.1038/nrurol.2014.53.
[54] S. Alimperti, H. You, T. George, S.K. Agarwal, S.T. Andreadis, Cadherin-11 regulates both mesenchymal stem cell differentiation into smooth muscle cells and the development of contractile function in vivo, J. Cell Sci. (12) (2014) 2627–2638, https://doi.org/10.1242/jcs.134833.
[55] E.J. Gonzalez, T.J. Heppner, M.T. Nelson, M.A. Vizzard, Purinergic signalling underlies transforming growth factor-β-mediated bladder afferent nerve hyperexcitability, J. Physiol. (13) (2016) 3575–3588, https://doi.org/10.1113/JP272148.
[56] R.L. Heise, A. Parekh, E.M. Joyce, M.B. Chancellor, M.S. Sacks, Strain history and TGF-β1 induce urinary bladder wall smooth muscle remodeling and elastogenesis, Biomech. Model. Mechanobiol. 2 (2012) 131–145, https://doi.org/10.1007/s10237-011-0298-y.
[57] L. Leiria, F. Mónica, F. Carvalho, M. Claudino, C. Franco-Penteado, A. Schenka, A. Grant, G. De Nucci, E. Antunes, Functional, morphological and molecular characterization of bladder dysfunction in streptozotocin-induced diabetic mice: evidence of a role for L-type voltage-operated Ca^{2+} channels, Br. J. Pharmacol. 163 (2011) 1276–1288, https://doi.org/10.1111/j.1476-5381.2011.01311.x.
[58] S. Pençe, E. Özbek, N. OzanTiryakioğlu, N. ErsoyTunali, H.H. Pençe, H. Tunali, rs3918242 variant genotype frequency and increased TIMP-2 and MMP-9 expression are positively correlated with cancer invasion in urinary bladder cancer, Cell. Mol. Biol. (9) (2017) 46–52, https://doi.org/10.14715/cmb/2017.63.9.9.
[59] S.S. Shin, S.Y. Won, D.H. Noh, B. Hwang, W.J. Kim, S.K. Moon, Morin inhibits proliferation, migration, and invasion of bladder cancer EJ cells via modulation of signaling pathways, cell cycle regulators, and transcription factor-mediated MMP-9 expression, Drug Dev. Res. (2) (2017) 81–90, https://doi.org/10.1002/ddr.21377.